Multiscale Bone Damage

Subjects: Engineering, Biomedical | Engineering, Mechanical

Contributor: Federica Buccino

The investigation of bone damage processes is a crucial point to understand the mechanisms of age-related bone fractures. In order to reduce their impact, early diagnosis is key. The intricate architecture of bone and the complexity of multiscale damage processes make fracture prediction an ambitious goal.

age-related bone fractures | multiscale imaging | bone damage | computational models | experimental validation

1. Imaging Techniques for Multiscale Damage Assessment and Prediction

The use of imaging techniques enables researchers to understand bone damage at different hierarchical scales. It is particularly relevant in the comprehension of the implications of fracture processes in the deterioration of bone quality. This section presents an overview of the available imaging techniques (Figure 1) to visualize bone morphologies, to assess bone fractures and to predict the fracture risk from the macro-scale to the nano-scale. The macro-architecture is currently evaluated by means of common clinical images. At lower hierarchical levels, the identification of damage processes is more complex and requires higher-resolution techniques.

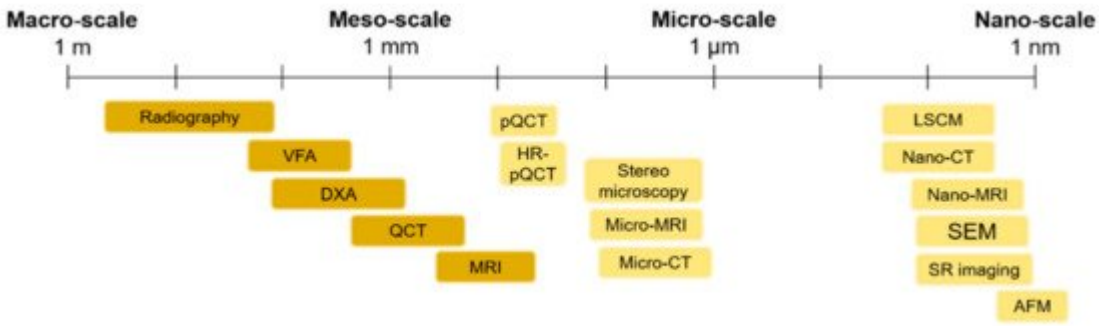

Figure 1. An overview of the main imaging techniques to assess bone damage at different scales. Macro- and meso-scale techniques are depicted in a darker color, while micro- and nano-scale imaging techniques are represented in a brighter color. VFA: Vertebral Fracture Assessment; QCT: Quantitative Computed Tomography; MRI: Magnetic Resonance Imaging; pQCT: peripheral Quantitative Computed Tomography; Micro-CT: Micro Computed Tomography; LSCM: Laser Scanning Confocal Microscopy; SEM: Scanning Electron Microscopy; SR imaging: Synchrotron Radiation imaging; AFM: Atomic Force Microscopy.

Different techniques are compared in terms of outcomes, in vitro or in vivo applications, resolution, two- or three-dimensional features and the main advantages and disadvantages.

1.1. Macro- and Meso-Scale Imaging

Table 1 shows the principal macro-scale techniques for the imaging of bone fractures and for fracture risk prediction.

Table 1. Overview of the main macro- and meso-scale imaging techniques.

Macro- and Meso-Scale Imaging Technique	Brief Description of the Technique	Invasiveness	Outcomes	Spatial Resolution	2D or 3D In Vitro/In Vivo Application	Advantages	Disadvantages
Radiography	Based on the interaction between a beam of photons (X-rays) directed from a source to a receptor. The atoms of the body prevent, in a percentage dependent on their atomic number, some photons from reaching the receptor, reproducing a "negative" image of the body	No Radiation dose: 40–50 times lower, if compared to computed tomography (CT) scans (e.g., radiographs of the abdomen → 0.25 mGy) [1]	Estimation of density variation (fracture risk prediction) by means of two indexes: Singh index [2] for proximal femur and cortical–medullary index [3] for hand radiographs	0.17 mm/pixel → The size of the monitor screens used in digital radiography is sufficient for 35 × 43 cm^2 radiographs to be displayed at a resolution of 2048 × 2560 pixels [4]	2D In vivo	Clear identification of distal radius fractures [5]	Difficult detection of hip and spine fractures Insensitive to changes in Bone Mineral Density (BMD)until 20 to 40% of bone mass lost [5]
Dual-energy X-ray Absorptiometry (DXA)	Involves the emission of two X-ray beams with different energy levels, that collide with the body of the patient. Once the absorption of the soft tissue has been	No Low radiation dose (0.001–0.003 mGy for L-spine, to 0.004 mGy for total body) [6]	Determination of areal BMD in g/cm^2 Calculation of bone mineral content (BMC = BMD × area) Calculation of T-score and	1 pixel → ≃ 0.56 × 0.56 mm^2. (for a Hologic system) [7]	2D In vivo	Ease of use of the equipment Standardization Short examination time [8]	No bone architecture detection (no difference between cortical and trabecular bone) Sampling errors Incorrect

Macro- and Meso-Scale Imaging Technique	Brief Description of the Technique	Invasiveness	Outcomes	Spatial Resolution	2D or 3D In Vitro/In Vivo Application	Advantages	Disadvantages
	subtracted, it is possible to determine the absorption of the beam by the bone and therefore the BMD		Z-score (negative for values under the average BMD), that are numerical indexes for the evaluation of osteoporosis.				evaluation in obese patients [6]
Vertebral Fracture Assessment (VFA)	Special DXA analysis that permits the detection of spinal fractures from a lateral image of the spine	No Lower radiation exposure with respect to spine radiography [9]	Spinal fracture detection [10]	Low spatial resolution	2D In vivo	Possibility to add a VFA scan after areal BMD assessment High sensitivity High specificity [11]	Low spatial resolution
Quantitative Computed Tomography (QCT)	X-ray-based technique that measures BMD. It produces cross-sectional images of X-ray absorption coefficient (measured in Hounsfield units) calibrated to water. It is used to evaluate fracture risk primarily at the lumbar spine and at the hip [12]	Medium–high invasiveness Medium–high radiation dose (0.2–0.4 mGy for a spine exam) [13]	True measurement of BMD assessment (areal BMD does not predict if an individual patient will eventually fracture)	100× higher resolution with respect to conventional radiologic imaging [14]	3D (multiple slices are obtained and then reconstructed) In vivo	Fracture risk prediction in patients with scoliosis, obesity, etc. without having artificially high BMD values, as in DXA [15] High reproducibility Assessment of cortical and trabecular bone Good accuracy and precision [6]	Relevant radiation dose Low accessibility High cost [16]
Magnetic Resonance Imaging (MRI)	MRIs employ a magnetic field that forces protons	No MRI does not use	Bone fracture detection Parameters:	MRI scanners used for medical	3D	Useful in age-related fracture detection (marrow fat	Presence of a magnetic field (risk for patients with

Macro- and Meso-Scale Imaging Technique	Brief Description of the Technique	Invasiveness	Outcomes	Spatial Resolution	2D or 3D In Vitro/In Vivo Application	Advantages	Disadvantages
	in the body to align with that field. When a radiofrequency current is pulsed through the patient, the protons are strained against the pull of the magnetic field.	ionizing radiation	T2* [17] (effective transverse relaxation time) → a function of the density and orientation of the trabeculae [18] R2* → rate	purposes could reach typical resolutions of around 1.5 × 1.5 × 4 mm^3 [20]		increases with age and in osteoporosis, allowing better contrast with the trabecular bone) Investigation of cortical water content [5]	pacemakers and all implants containing iron) Noise up to 120 dB Use of contrast agents

Micro- and Nano-Scale Imaging Technique	Brief Description of the Technique	Invasiveness	Outcomes	Spatial Resolution	2D or 3D In Vitro/In Vivo Application	Advantages	Disadvantages
Stereomicroscopy Based on Histological Sections	Histology from the bone tissue is obtained and then the sample is properly treated (fixation, dehydration and clearing, embedding, sectioning, staining and mounting). The histological section is then observed by means of an optical microscope	Yes	Traditional technique for the visualization of bone microarchitecture	~1.6 µm [21]	2D In vitro	Bone remodeling assessment [22]	Destructive and invasive technique Limitations related to the bidimensional output images: the three-dimensional features are lost. High-resolution images (at least 1.4 µm or better) are required to identify and measure individual resorption cavities in the process of bone remodeling [22]
Micro-Computed Tomography (Micro-CT) and Nano-Computed Tomography (Nano-CT)	Micro- and nano-CT scans use radiographs to generate cross-sections of bone, that are generally processed	No Generally, the samples are obtained from surgical wastes that derive from	Microarchitectural 3D data for both the cortical and the trabecular sections (tissue volume, bone volume, bone surface, bone volume fraction,	1.2 µm (micro-CT) ~50–150 nm (nano-CT)	3D	Large number of obtainable outputs (morphological parameters at different scales) Detailed finite	Static evaluation of micro-scale features Not suitable for in vivo human evaluation due

ture risk

Micro- and Nano-Scale Imaging Technique	Brief Description of the Technique	Invasiveness	Outcomes	Spatial Resolution	2D or 3D In Vitro/In Vivo Application	Advantages	Disadvantages
	(image reconstruction) to generate a virtual 3D model without destroying the original bone sample	prosthetic treatment	bone surface to tissue volume, trabecular/cortical thickness, degree of anisotropy, cortical porosity, etc.) [6]. Local and global parameters related to the lacunar network are obtained [23]		In vitro	element 3D models could be implemented by using micro-CT images	to the high radiation dose No detection of the canalicular network (insufficient resolution for the micro-CT scans) Nano-CT
Peripheral QCT (pQCT) and High-Resolution pQCT (HR-pQCT)	Dedicated CT scanners for the forearm (radius and ulna) and leg (tibia and fibula)	No Low radiation dose (≈0.003 mGy) [6]	Analysis of the trabecular and cortical sections (BMD, bone mineral content and bone geometrical parameter calculation). Acquisition of biomechanical parameters, such as the cross-sectional moment of inertia. Evaluation of the functional muscle–bone unit [24].	Isotropic voxel size of 82 µm with HR-pQCT	3D In vivo	High precision and accuracy Low radiation dose Applicable for the study of a large number of diseases, especially pediatric (useful in applications where trabecular and cortical sections are affected in a different way)	Evaluation restricted to the appendicular bone Only transversal data are available for fracture risk prediction Low spatial resolution
Synchrotron Radiation Imaging (SR)	A high-intensity white beam travels around a fixed closed loop. It permits a high level of detail in bone visualization (ultra-structural porosity detection)	No Generally, the samples are obtained from surgical wastes that derive from prosthetic treatment	Morphological analysis of ultra-structural porosities	Voxel size of 0.9 µm for the white beam [25]	3D In vitro	Visualization of the lacunar and canalicular network Phase contrast permits the clear detection of micro-cracks	Reduced field of view

Micro- and Nano-Scale Imaging Technique	Brief Description of the Technique	Invasiveness	Outcomes	Spatial Resolution	2D or 3D In Vitro/In Vivo Application	Advantages	Disadvantages
Micro-MRI and nano-MRI	The technique generates images by exploiting the nuclear magnetic behavior of different atoms in a sample tissue placed in a magnetic field	No	Structural parameters, such as trabecular bone thickness and mean bone volume fraction, associated with bone biomechanical properties and fracture resistance	Spatial resolution up to 25 µm (micro-MRI) and ~10 nm for the nano-MRI	3D In vivo	Non-destructive technique Good special resolution Good contrast resolution [26]	Long acquisition times High costs [26]
Laser Scanning Confocal Microscopy (LSCM)	LSCM employs lasers at proper wavelengths to excite fluorochromes that are used to stain bone sections	Yes	Correlation between micro-crack parameters and bone matrix toughness Comparison among damage morphologies [27]	180 nm laterally and 500 nm axially [28]	2D/3D images of consecutive planes can be reconstructed into a 3D image in vitro.	Evaluation of bone microdamage	Axial resolution in depth impaired by spherical aberration [28] High costs
Scanning Electon Microscopy (SEM)	SEM produces images of the bone sample by scanning the surface with a focused beam of electrons	Yes	Quantitative analysis of fracture surfaces Visualization of microdamage morphology, fiber bridging and interlamellar separation [27]	~1 nm	3D In vitro	Significant information related to sub-micro-scale damage	Destructive technique (sample surfaces should be conductive → bone needs to be coated with conductive materials)
Atomic Force Microscopy (AFM)	The deflections of a cantilever on the surface of the bone sample are transduced into electrical signals	Yes	Topographical parameters of fractured bone surfaces (mineral particle sizes) Identification of sacrificial bonding	Vertical resolution → up to 0.1 nm Lateral resolution → ~30 nm	3D In vitro	Versatile imaging technique for the visualization of fracture surfaces High accuracy Non-	Small dimensions of the single scan image size (150 × 150 µm, compared with mm for SEM) Slow

al in the physical ported in Table 1), rts. The e, which mputed hich the imaging to point end their ossibility roscopy. ensional from a damage e and to tation of e, micro-ion (SR) images. They provide, in fact, a three-dimensional reconstruction of bone micro-architecture, which is important for the identification of microdamage, offering the optimal balance between resolution and field of view. In addition to this, the SR technique is a promising solution for the real-time visualization of bone damage, allowing the performance of mechanical tests inside the synchrotron facility. The disruptive advent of these high-resolution in vitro techniques offers the possibility to experimentally validate numerical damage models, as deeply discussed in the section “Validation approaches to multiscale damage models”. Additionally, these techniques could help the study of effective pharmacological treatments for bone pathologies. Current treatments, in fact, are administered just after an evident diagnosis of osteoporosis, often when patients have already undergone a severe fracture. Consequently, the possibility to correlate micro-scale fragility indexes with the current bone meso- and macro-

Micro- and Nano-Scale Imaging Technique	Brief Description of the Technique	Invasiveness	Outcomes	Spatial Resolution	2D or 3D In Vitro/In Vivo Application	Advantages	Disadvantages
						destructive technique [29]	

specific

2. Bone Damage Physical Principle

Imaging techniques are a valuable tool for the visualization of bone features and multiscale damage and could help in the comprehension of bone damage mechanisms. Due to the fact that bone is a hierarchical material with multiple linked scales, bone fracture mechanisms also occur at the multiscale. Those mechanisms are particularly complex and not completely understood.

At the macro-scale, there are essentially two main bone fracture modalities: impact fracture and stress fracture. The former is a fracture caused by an overload, while the latter is associated with cyclic loading and it causes material failure by excessive damage accumulation [30][31]. Stress fractures include both fatigue fractures, which result from strong physical activity, and fragility fractures, which are consequences of everyday common activities. The latter are often linked to age-related decreases in bone's ability to self-repair. This often happens in age-related bone pathologies such as osteoporosis. At the macro-scale, the shape, size and density of bone strongly affect fracture behavior [29].

At the meso-scale, trabecular bone microarchitecture influences the damage. Trabecular bone is subjected to a variety of loads during activities of daily life and the orientation of the applied load with respect to the trabecular distribution plays an important role in a possible trabecular tissue degeneration. Indeed, trabeculae generate a three-dimensional, open porous space. Pathologies such as osteoporosis may lead to a conversion from a plate-like to a rod-like trabecular morphology, which contributes to increasing the fracture risk [32]. Typically, trabecular failure initiates at the weakest trabecula or at the weakest trabecular region. From there on, the failure will progress and failure bands will develop. During a tensile test, there will be only one failure band; multiple failure bands, however, occur in compressive tests [33]. Gibson [34] investigated how the basic failure modes (bending, compression, tension, shear) can explain trabecular bone failure (Figure 2). It has been also observed that complete fractures are present in trabeculae that are oriented transversally to the direction of the applied load [35].

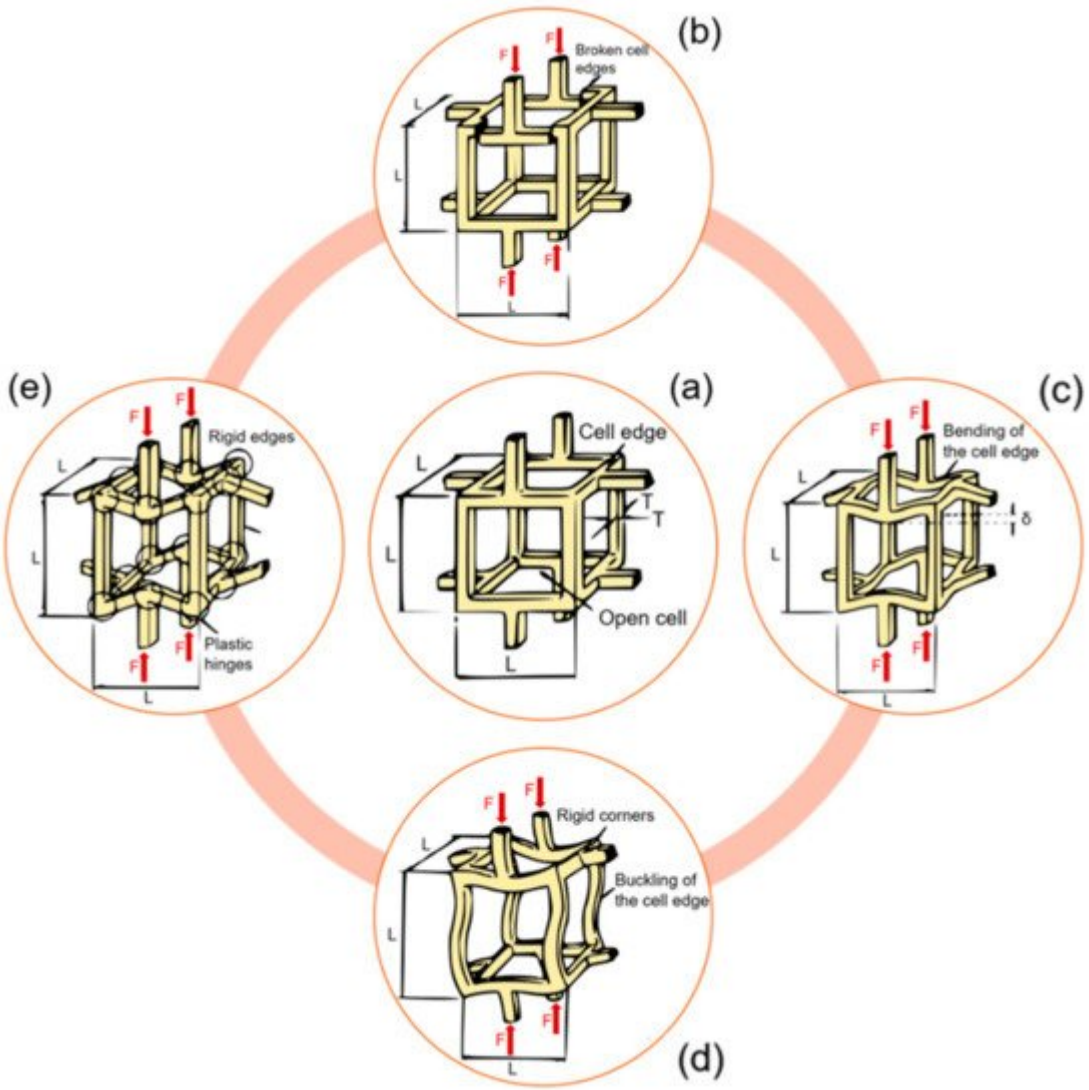

Figure 2. Different meso-scale failure modes of a trabecular network. (**a**) An unloaded trabecular cell. (**b**) Brittle crushing. (**c**) Bending of horizontal rods, compression of vertical rods. (**d**) Buckling of vertical rods, bending of horizontal rods. (**e**) Plastic yielding. Readapted from [34].

At the micro-scale, a complete comprehension of the bone damage physical principle is still lacking. Bone is able to sustain many micro-cracks, if they are not critical; this suggests that bone can be classified as a “damage-tolerant material” [36]. This concept is particularly interesting when applied to bone microstructure. At the micro-scale, the damage assumes two frequent morphologies: linear and diffuse damage. The linear damage appears as a sharp line of 100–200 µm [37] separating the bone matrix, and it is typical of regions subjected to compression [30]. When external compression boundary conditions are applied, linear cracks propagate parallel to the compression loading axis [38]. On the contrary, diffuse damage is characterized by a cloud of tiny cracks [39], whose dimensions are less than 1 µm [37], and this is typical of regions subjected to tension. Diffuse micro-cracks are distributed transversally to the applied tensile stress [40]. Voide et al [41] suggest that diffuse damage could be considered as linear damage when oriented differently with respect to a global reference system. Micro-cracks occur on multiple planes when subjected to torsion or mixed-mode loading (Figure 3).

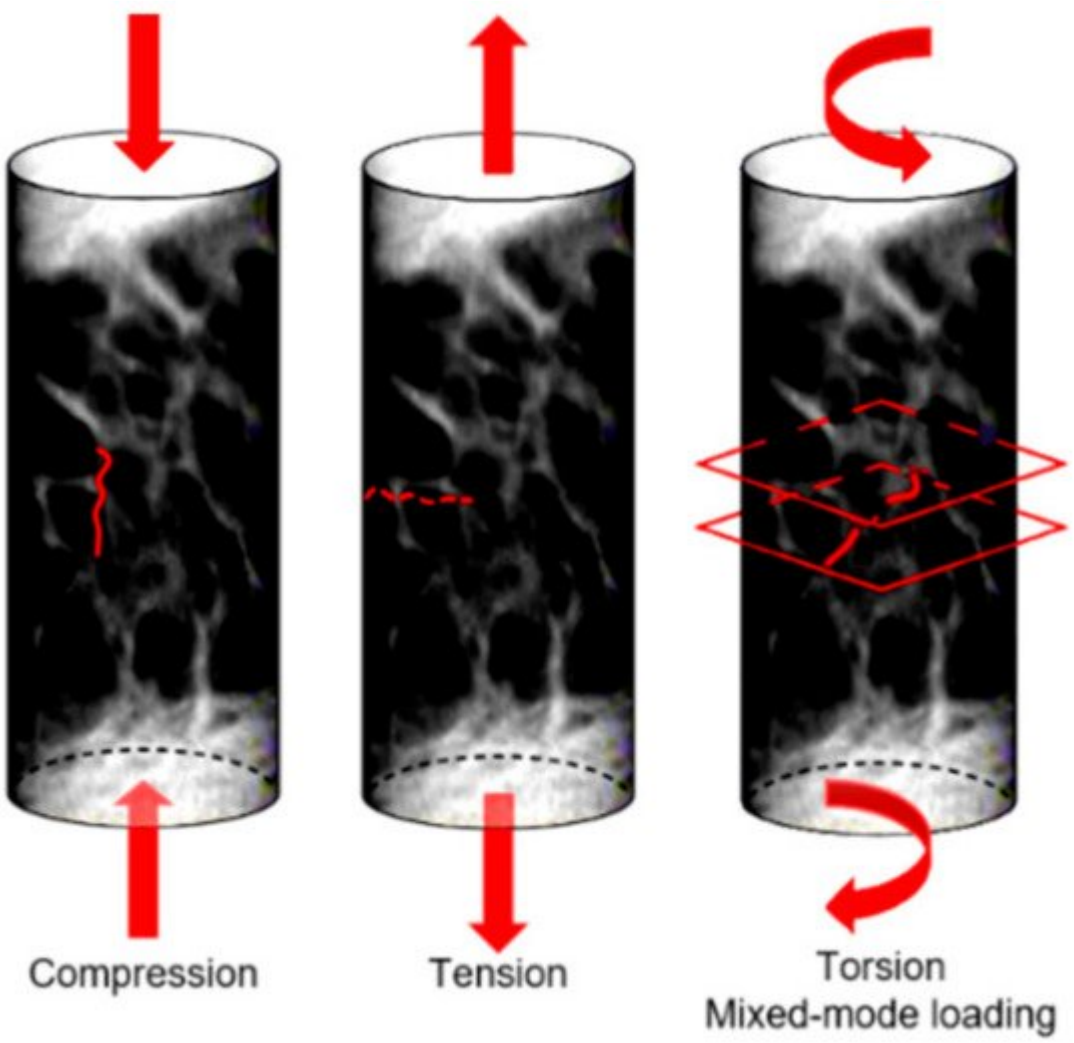

Figure 3. Orientation of micro-cracks in a bone sample subjected to different loading conditions.

Micro-cracks usually initiate at regions characterized by high stresses. As soon as the crack initiates, its growth behavior is influenced by micro-scale heterogeneities. In this context, particular interest has recently been devoted to cellular-level porosity represented by the lacunar network, whose role is still under debate. A variation in the lacunar distribution or in the lacunar shape, as happens with aging, significantly affects the bone resistance to fracture [42]. Lacunae play a dual mechanical role, having an effect on both strength and toughness. In the first instance, lacunae are stress concentrators [43], by representing bone discontinuities able to locally amplify stresses and strains. The average strain around lacunae is 1.5–4.5 times higher than the remote strain applied to the surrounding tissue [44][45]. In this sense, lacunar system should contribute to strength decreases.

However, considering bone as a damage-tolerant material, experimental investigations [41] show that lacunae are not the starting point for the micro-cracks that ultimately lead to bone failure. Micro-cracks nucleate generally at canals [41] or at cement lines and inter-lamellar zones [46][47], where the stress amplification is greater than at the lacunae [48][49]. According to those investigations, lacunae make a beneficial contribution to toughness [38]. Voide et al. suggest that lacunae exert an attraction upon the existing micro-crack: the deviation of the crack path reduces the energy of its progression, slowing down crack propagation [50]. The two effects of the lacunar network are

schematized in Figure 4. The role of the lacunar network still needs to be clarified by an effective experimental validation of the proposed hypotheses.

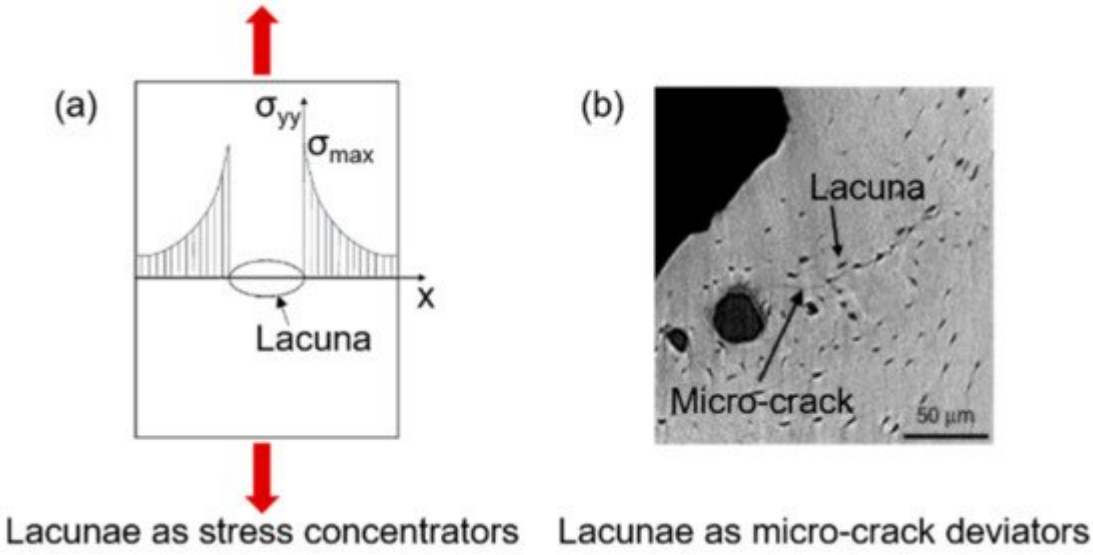

Figure 4. The dual effect of the lacunar system on microdamage: lacunae as sites for crack initiation (**a**) and lacunae as micro-crack deviators (**b**); (**b**) is adapted from [38].

Finally, at the nano-scale, bone failure and fracture are influenced by bone's composition in terms of hydroxyapatite and collagen fibers. Hydroxyapatite minerals show a brittle behavior and are more resistant to compression, while collagen fibers are more resistant to tension. When the crack propagates, the hydroxyapatite will fail first and the complete failure only occurs when collagen fibers are fully stretched [51].

It is understood how the comprehension of the bone damage physical principle at the multiscale level is a crucial point for the implementation of computational damage models. Those models have recently attracted a high degree of interest [52], due to the fact that patient-specific simulations, in particular in this context of age-related bone fractures, allow a more accurate prognosis [53][54]. The ability to quantify the effects of aging and pathologies such as osteoporosis is a challenging issue that computational damage models should consider.

3. Multiscale Computational Damage Models

Given that macro- and micro-architecture play an important role in bone damage and crack propagation, computational analyses can be interesting tools to investigate the effect of their variation due to aging on bone fractures. Using finite element (FE) models, generated directly from micro-CT or synchrotron images, it is possible to perform a "virtual experiment", able to simulate mechanical loading of the sample and to evaluate damage formation. The main advantage of FE models is that, once the geometry of the structure is implemented, the same model can be used for multiple analyses, i.e., applying different loading conditions that may mimic everyday life loadings (e.g., walking, running).

Furthermore, bone FE models provide new insight into the relationship between damage propagation and macro- and micro-scale architecture, by allowing the localization of zones that are more prone to fracture. While in the past FE models were limited by input image resolution and computational power [53], nowadays, accurate simulations are feasible, thanks to the recent developments in imaging and in optimized computational software. The increased accuracy of bone FE damage models demonstrates that computational simulations are a reliable way to improve the choice of more effective experimental tests, potentially leading to a reduction in the number of performed tests [55][56].

In this section, both macro- and micro-scale models are presented, with an attempt to investigate bone fracture initiation and propagation at different scales [57].

Macro-scale organ-level models primarily focus on the effects of mechanical stimuli on bone resistance to fracture. Those models, that start mainly from CT reconstructions, try to implement the observation of J. Wolff [58], related to bone's capability to adapt to the external mechanical loading conditions [59]. At this scale, micro-architectural features are neglected. The outer shape object of the problem is simplified, and filled with different meshing strategies, for instance, geometry-based with tetrahedral elements, or voxel-based with hexahedral elements. While the first method, that requires a smaller number of degrees of freedom, is not fully automated, the voxel-based hexahedron meshing has no geometrical limitations and it is a fast and completely automated mesh generation technique [60]. However, in the second case, outer surfaces or sharp geometrical discontinuities may generate a lack of convergence. Generally, the voxel-based meshing strategy allows a simpler and more effective interface with CT scans. The bone material is typically considered as a continuum solid [61]. The model is loaded with defined boundary conditions (compression, torsion or mixed-mode loading). The external load produces local stresses and strains in each considered element of the mesh (Figure 5), which could be correlated by means of the constitutive equation [62]. The constitutive equation, in the condition of linear elasticity, provides a linear relation between stresses and strains by means of the mechanical properties of the bone tissue, assuming the strains to be small or infinitesimal [63].

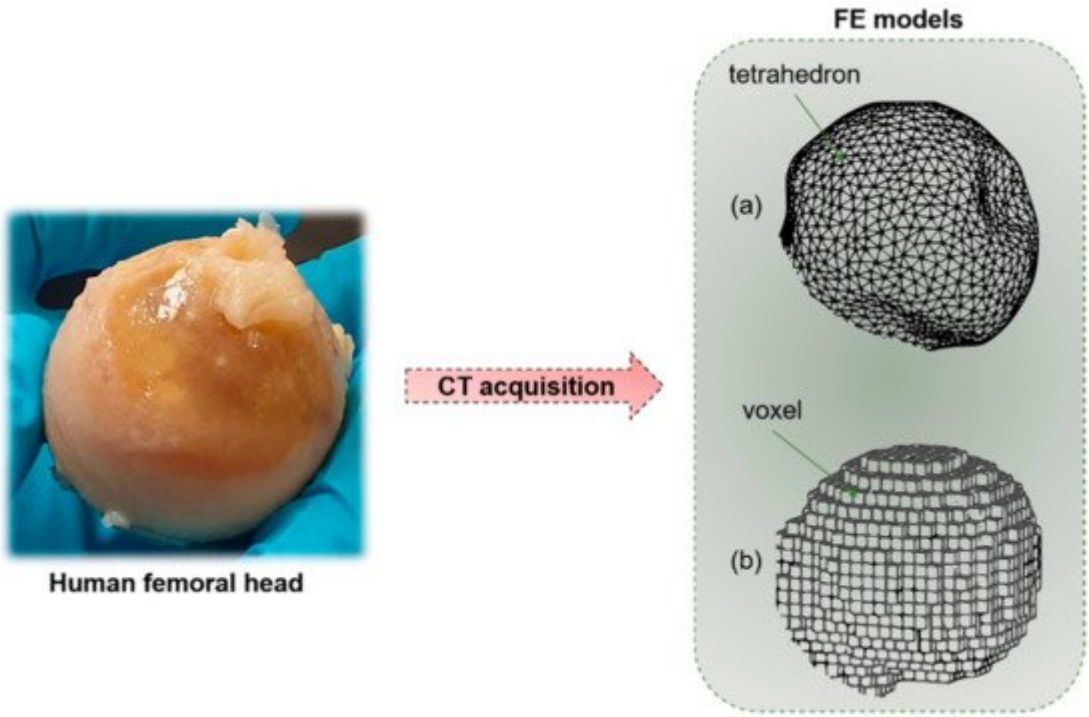

Figure 5. Starting from a human bone (e.g., femoral head), by means of CT acquisition, it is possible to obtain a macro-scale finite element (FE) model of the sample. (**a**) Geometry-based FE models with tetrahedral elements. (**b**) Voxel-based FE model with hexahedral elements.

The initiation and propagation of damage in the macro-scale bone model is defined according to a proper failure criterion [64]. Based on the theory of elasticity, those models generally assume that bone resorption occurs when local mechanical stress overcomes a homeostatic stress state [65]. In the definition of failure at the macro-scale, it should be considered that local tissue failure could provide a loss in the structural integrity. The main results of macro-scale models, as reported in the scheme of Figure 6, show that subject-specific FE models predict values of strain with an accuracy of 90%, obtained by comparison with experimental measurements on cadaver bones (the average errors on surface strains are lower than 10%) [66]. The encouraging results are due to the coexistence of a precise geometric reconstruction, an appropriate choice of the density–elasticity relationship, an accurate application of boundary conditions and a suitable algorithm for material property evaluation.

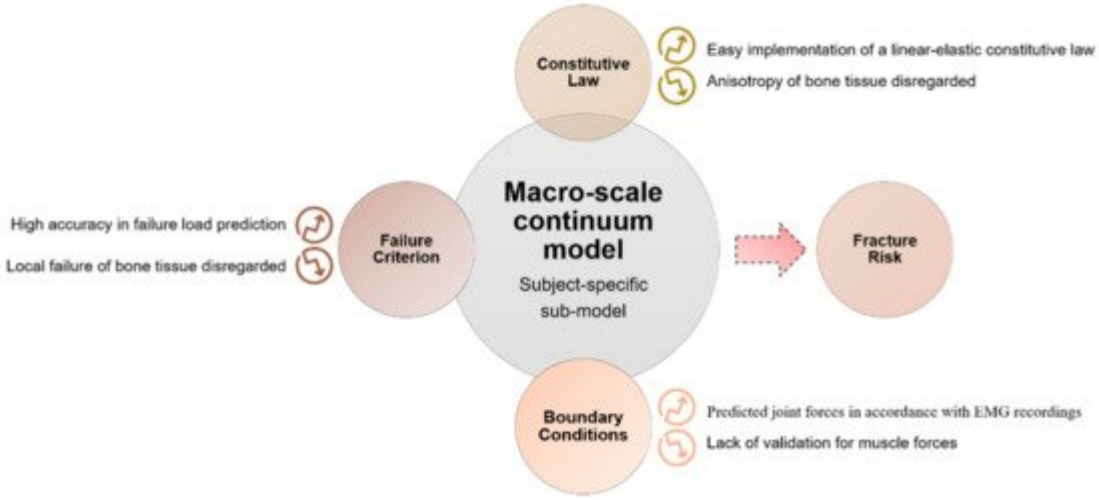

Figure 6. Scheme for the implementation of a whole-bone model. Results, potentialities and limitations are highlighted for each step. EMG: Electromyography.

A relevant aspect of macro-scale models is that they can consider an accurate map of the tissue elastic modulus distribution, based on the density distribution over the continuum bone model, as performed by Viceconti [64] and Taddei [67]. These models show low average error in predicting failure load in vitro and have a high precision in identifying the location of failure [64].

Further attempts in macro-scale FE modes have been performed in order to capture the non-linear behavior of bone that depends both on the anatomic site and the loading mode. In particular, Imai et al. [68] observe that the prediction of vertebral fracture is intricate due to the complex geometry of the vertebra and its elastoplasticity. They implement non-linear FE models of the whole vertebra; in order to consider bone heterogeneity, the mechanical properties of each element are computed from the Hounsfield unit value. The correlation between the measured value of fracture strength and the predicted values with the non-linear FE models shows significant improvements [68] with respect to previous linear and simplified FE models. Other attempts in modeling bone failure have been performed by Harrison et al. [69], considering that the tissue failure consists of two phases: damage and fracture. This study develops a computational model consisting of an explicit representation of complete failure, incorporating non-linear damage criteria, fracture criteria, cohesive forces, asymmetry and large deformation capabilities.

However, those models are not able to capture patient-specific cortical nor trabecular micro-architecture, which play a crucial role in bone strength [69][70][71].

Micro-scale models provide further insights into bone fracture prediction at smaller scales. Traditionally, micro-architectural features were assessed by means of histological sections [72] that lack in three-dimensionality. Nowadays, the input of micro-scale models often comes from micro-CT or SR images, that have a resolution able to non-destructively capture not only trabecular architecture, but even ultrastructural porosities, such as lacunae. However, this corresponds to higher computational costs, calculated by van Rietbergen et al. [73] through an element-by-element method that implies the use of uniformly shaped elements to reduce memory allocation and

optimize computational times. Some issues arise when dealing with micro-CT or SR imaging techniques: filtration and segmentation. Reconstructed image data include noise that should be removed or at least reduced by filtering. The choice of an adequate filter (the Gaussian filter is the most suitable one, which is easily implementable and fast in computation [74]) is essential in order to obtain an input image for the model, as close as possible to the original sample. Another relevant aspect is the correct segmentation process that selects those voxels that are below or above a defined threshold, so as to separate those elements that are bone and those that can be considered as voids. This distinction is particularly relevant when dealing with the identification of micro-cracks and lacunae, whose typical size is significantly smaller (about 10 µm [38]) with respect to the trabecular architecture. Micro-FE models are often used for the prediction of bone fracture. For this purpose, specific damage criteria are implemented. In the work of Pistoia et al. [75], a micro-FE linear analysis is performed on the human distal radius. In order to predict bone failure, the chosen criterion is that the bone failure initiation occurs when bone is strained beyond a critical value, defined as the yield strain. This model is able to give a better prediction of bone failure loads (R^2 = 0.75 correlation with experimental testing) with respect to macro-scale investigation techniques such as DXA measurements. Linear micro-FE models are also proposed for the study of the interaction between micro-cracks and micro-porosities, such as lacunae or surface discontinuities in bones. The role of the lacunar network in damage initiation and propagation is still unclear, due to the difficulty in obtaining dynamic visualization of the advancing crack. Micro-FE models shed some light on micro damage initiation and propagation. In this context, it is necessary to define a proper descriptor of the stress distribution, such as the strain energy density (SED) or the maximum principal stress (σ_1) criteria. SED is a good predictor for the mechanical environment sensed by the osteocytes that reside in lacunae [76] and σ_1 is a mechanical quantity often used to assess the failure in brittle materials [77]. Those two criteria show different sites of crack initiation and different directions for crack propagation (Figure 7).

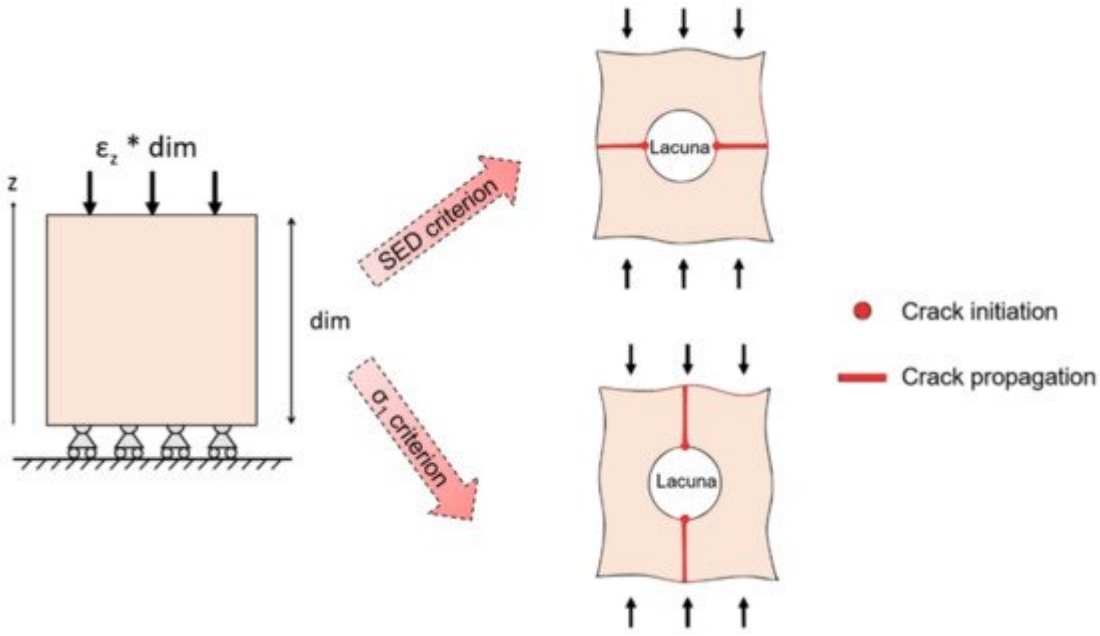

Figure 7. Schematic output of models of a bone sample with a lacuna subjected to compression. Crack initiation (dots) and crack propagation (lines) are highlighted, according to strain energy density (SED) damage criterion and

to σ_1 criterion.

The σ_1 criterion locates peak stresses and strains at regions matching with the experimental initiation stresses and strains found by Voide et al. [41]. Donaldson et al. [77] compare different linear micro-FE models that aim at the identification of crack initiation sites and of the role of the lacunar network. They present a relevant novelty by implementing a stress gradient model, schematized in Figure 8, that shows a clear directionality in the advancing crack (instead of the less realistic stress limit algorithm, that is able to simulate only accumulated damage around voids or surface discontinuities).

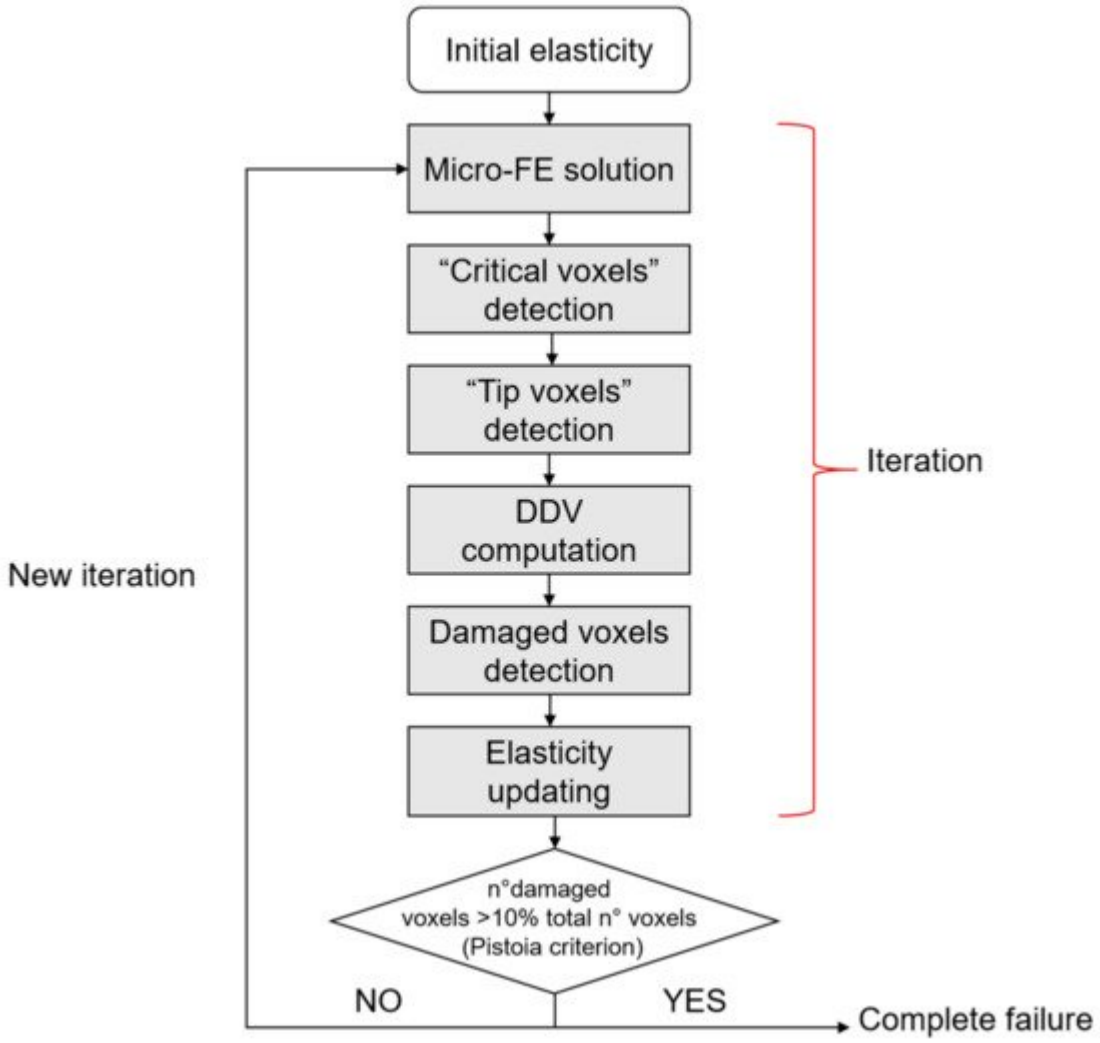

Figure 8. Stress gradient algorithm. "Critical voxels" are the voxels that exceed a defined stress threshold. "Tip voxels" are the center of the spherical sensation region of the osteocytes and are eligible sites for damage propagation. In the stress gradient algorithm, a key role is played by the deletion direction vector (DDV), that indicates a direction for crack propagation. The iteration stops when the total failure of the sample is reached, according to the Pistoia criterion [75].

The stress gradient algorithm clarifies that damage starts from surface discontinuities or blood vessel (Figure 9) and not from lacunae, confirming from a computational point of view the hypothesis.

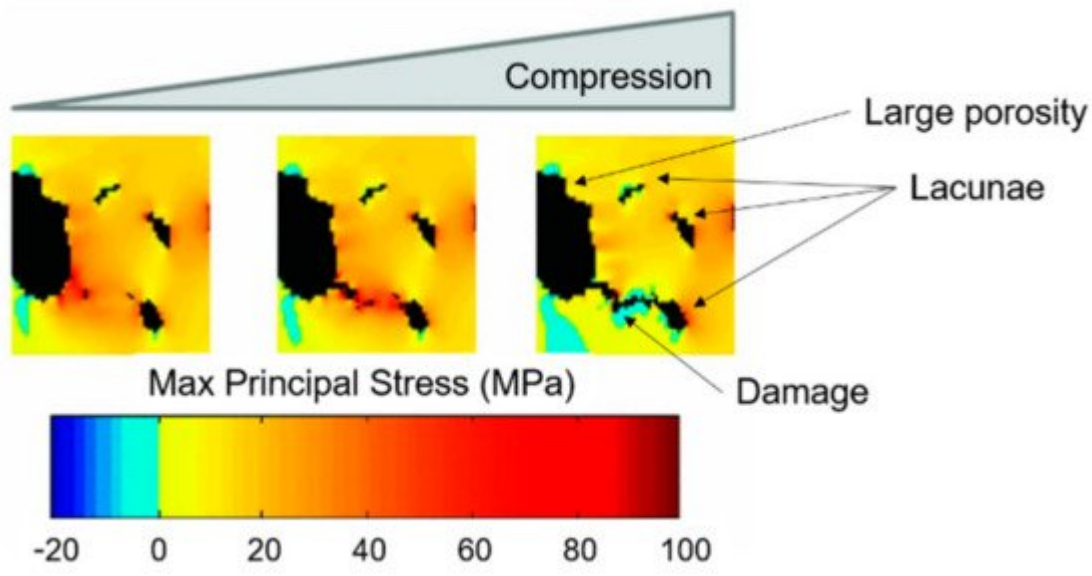

Figure 9. Stress gradient algorithm (on SR CT data from a cortical bone sample) results: damage starts from big porosities and its propagation follows the stress gradient. Micro-damage is deviated by the presence of lacunae. Readapted from [77].

Despite the explained potentialities of linear micro-FE damage models, micro-damage predictions could be improved by implementing the bone non-linear behavior. The experimental tests focused on non-linear bone properties indicate ductile failure modes [78], in which damage is combined with the plasticity component of collagen fibers [79]. Hammond et al. [80] perform non-linear FE models (in this case, material non-linearity is considered) on trabecular samples from the distal femur of a human cadaver. They consider two micro-crack formation criteria, one for isotropic tissue models and one for anisotropic tissue models. For the isotropic tissue models, micro-cracks initiate if the ratio between maximum tensile principal stress and micro-crack initiation strength is equal to one. For anisotropic tissue models, micro-damage initiates if the maximum ratio between the normal of shear tractions with respect to the micro-crack initiation strength is equal to one. This non-linear micro-FE model is able to demonstrate that the anisotropy of bone tissue significantly contributes to bone fracture resistance [81]. Stipsitz et al. [82] try to implement an efficient micro-FE solver for large-scale non-linear simulations. However, the non-linearity of the system makes the results highly dependent on small structural deviations introduced by coarsening the structure. Additionally, one of the main drawbacks of the use of non-linear models is the increased computational cost, almost 10 times higher than linear simulations [53].

An increased degree of complexity can be found when analyzing nano-scale damage models that require further understanding of the variations in chemical pathways due to aging or disease. The first attempts in nano-scale bone fracture modeling were performed by Dubey et al. [83]: in their study, bone tissue fracture properties are based on the atomistic strength analyses of type I collagen in combination with hydroxyapatite interfacial arrangement, using molecular dynamics. Additional nano-scale studies [84] reveal that a decrease in the hydroxyapatite crystal size may change the mechanical behavior of the whole bone and the failure mode: from brittle-like crack-driven failure in larger crystals to a more widespread failure mode in the smaller ones. However, heterogeneities at the nano-scale remain difficult to model in a constitutive law and their role and effects are still unknown [85]. The

impossibility to perform direct experimental tests on bone samples at the nano-scale is also a reason why those models are less considered for the purpose of this review.

To summarize, the increased image resolution and the optimization of parallel computational architecture for the solving of FE damage models seem promising tools for the improvement of the clinical understanding of fracture risk prediction. It is necessary to point out that some attempts in performing multiscale analyses have been performed by implementing bottom-up multiscale approaches, starting from the nano-scale up to the meso-scale [86] and analogously by Kwon et al. [87], who apply the multiscale analysis with variable geometrical parameters in order to determine its effect on the bone properties.

Before translating in silico damage models to clinical practice, the essential step is the experimental validation of the mentioned models that are still in their infancy, especially at smaller scales.

References

1. Al-Lamki, L. Radiation Exposure from Medical Imaging: A Wake-up Call for Oman! Sultan Qaboos Univ. Med. J. 2011, 11, 1–4.
2. Singh, M.; Nagrath, A.R.; Maini, P.S. Changes in trabecular pattern of the upper end of the femur as an index of osteoporosis. J. Bone Joint Surg. Am. 1970, 52, 457–467.
3. Bouxsein, M.L.; Palermo, L.; Yeung, C.; Black, D.M. Digital X-ray radiogrammetry predicts hip, wrist and vertebral fracture risk in elderly women: A prospective analysis from the study of osteoporotic fractures. Osteoporos. Int. 2002, 13, 358–365.
4. Huda, W.; Brad Abrahams, R. X-ray-based medical imaging and resolution. Am. J. Roentgenol. 2015, 204, W393–W397.
5. Bilezikian, J.; Raisz, L.; Martin, T.J. Principles of Bone Biology, Two-Volume Set, 4th ed.; Elsevier: Amsterdam, The Netherlands, 2008; Volume 1–2, ISBN 9780123738844.
6. D'Elia, G.; Caracchini, G.; Cavalli, L.; Innocenti, P. Bone fragility and imaging techniques. Clin. Cases Miner. Bone Metab. 2009, 6, 234–246.
7. Morris, R.M.; Yang, L.; Martín-Fernández, M.A.; Pozo, J.M.; Frangi, A.F.; Wilkinson, J.M. High-Spatial-Resolution Bone Densitometry with Dual-Energy X-ray Absorptiometric Region-free Analysis. Radiology 2015, 274, 532–539.
8. IAEA International Atomic Energy Agency. Dual Energy X-ray Absorptiometry—Bone Mineral Densitometry|IAEA. Available online: (accessed on 24 February 2020).
9. Zeytinoglu, M.; Jain, R.K.; Vokes, T.J. Vertebral fracture assessment: Enhancing the diagnosis, prevention, and treatment of osteoporosis. Bone 2017, 104, 54–65.
10. El Maghraoui, A.; Roux, C. DXA scanning in clinical practice. QJM 2008, 101, 605–617.

11. Schousboe, J.T.; DeBold, C.R. Reliability and accuracy of vertebral fracture assessment with densitometry compared to radiography in clinical practice. Osteoporos. Int. 2006, 17, 281–289.
12. Adams, J.E. Quantitative computed tomography. Eur. J. Radiol. 2009, 71, 415–424.
13. Brett, A.D.; Brown, J.K. Quantitative computed tomography and opportunistic bone density screening by dual use of computed tomography scans. J. Orthop. Transl. 2015, 3, 178–184.
14. Kim, T.Y.; Schafer, A.L. Bariatric Surgery, Vitamin D, and Bone Loss. In Vitamin D: Fourth Edition; Elsevier: Amsterdam, The Netherlands, 2017; Volume 2, pp. 129–150. ISBN 9780128099650.
15. Yu, E.W.; Thomas, B.J.; Brown, J.K.; Finkelstein, J.S. Simulated increases in body fat and errors in bone mineral density measurements by DXA and QCT. J. Bone Miner. Res. 2012, 27, 119–124.
16. Jahng, J.S.; Kang, K.S.; Park, H.W.; Han, M.H. The Assessment of Bone Mineral Density in Postmenopausal and Senile Osteoporosis Using Quantitative Computed Tomography. J. Korean Orthop. Assoc. 1990, 25, 262.
17. Link, T.M.; Majumdar, S.; Augat, P.; Lin, J.C.; Newitt, D.; Lane, N.E.; Genant, H.K. Proximal femur: Assessment for osteoporosis with T2* decay characteristics at MR imaging. Radiology 1998, 209, 531–536.
18. Yablonskiy, D.A.; Haacke, E.M. Theory of NMR signal behavior in magnetically inhomogeneous tissues: The static dephasing regime. Magn. Reson. Med. 1994, 32, 749–763.
19. Funke, M.; Bruhn, H.; Vosshenrich, R.; Rudolph, O.; Grabbe, E. Bestimmung der T2*-relaxationszeit zur charakterisierung des trabekularen knochens. RoFo 1994, 161, 58–63.
20. Van Reeth, E.; Tham, I.W.K.; Tan, C.H.; Poh, C.L. Super-resolution in magnetic resonance imaging: A review. Concepts Magn. Reson. Part A 2012, 40A, 306–325.
21. Nothnagle, P.; Chambers, W.; Davidson, M. Introduction to Stereomicroscopy. Available online: (accessed on 23 March 2020).
22. Vanderoost, J. From histology to micro-CT: Measuring and modeling resorption cavities and their relation to bone competence. World J. Radiol. 2014, 6, 643.
23. Mader, K.S.; Schneider, P.; Müller, R.; Stampanoni, M. A quantitative framework for the 3D characterization of the osteocyte lacunar system. Bone 2013, 57, 142–154.
24. Schoenau, E.; Neu, C.M.; Beck, B.; Manz, F.; Rauch, F. Bone mineral content per muscle cross-sectional area as an index of the functional muscle-bone unit. J. Bone Miner. Res. 2002, 17, 1095–1101.
25. Fedorov, A. Elettra Sincrotrone Trieste Elettra Sincrotrone Trieste. Available online: (accessed on 23 March 2020).

26. Liu, X.S.; Zhang, X.H.; Rajapakse, C.S.; Wald, M.J.; Magland, J.; Sekhon, K.K.; Adam, M.F.; Sajda, P.; Wehrli, F.W.; Guo, X.E. Accuracy of high-resolution in vivo micro magnetic resonance imaging for measurements of microstructural and mechanical properties of human distal tibial bone. J. Bone Miner. Res. 2010, 25, 2039–2050.
27. Poundarik, A.A.; Vashishth, D. Multiscale imaging of bone microdamage. Connect. Tissue Res. 2015, 56, 87–98.
28. Fouquet, C.; Gilles, J.F.; Heck, N.; Santos, M.D.; Schwartzmann, R.; Cannaya, V.; Morel, M.P.; Davidson, R.S.; Trembleau, A.; Bolte, S. Improving axial resolution in confocal microscopy with new high refractive index mounting media. PLoS ONE 2015, 10.
29. Dufrêne, Y.F. Atomic force microscopy, a powerful tool in microbiology. J. Bacteriol. 2002, 184, 5205–5213.
30. Acevedo, C.; Stadelmann, V.A.; Pioletti, D.P.; Alliston, T.; Ritchie, R.O. Fatigue as the missing link between bone fragility and fracture. Nat. Biomed. Eng. 2018, 2, 62–71.
31. Daffner, R.H.; Pavlov, H. Stress fractures: Current concepts. AJR Am. J. Roentgenol. 1992, 159, 245–252.
32. Taylor, D. Fracture and repair of bone: A multiscale problem. J. Mater. Sci. 2007, 42, 8911–8918.
33. Shi, X.; Liu, X.; Wang, X.; Guo, X.; Niebur, G.L. Type and orientation of yielded trabeculae during overloading of trabecular bone along orthogonal directions. J. Biomech. 2010, 43, 2460–2466.
34. Gibson, L.J. Biomechanics of cellular solids. J. Biomech. 2005, 38, 377–399.
35. Fyhrie, D.; Schaffler, M.B. Failure mechanisms in human vertebral cancellous bone. Bone 1994, 15, 105–109.
36. Zimmermann, E.A.; Busse, B.; Ritchie, R.O. The fracture mechanics of human bone: Influence of disease and treatment. Bonekey Rep. 2015, 4.
37. Vashishth, D. Hierarchy of bone microdamage at multiple length scales. Int. J. Fatigue 2007, 29, 1024–1033.
38. Voide, R.; Schneider, P.; Stauber, M.; van Lenthe, G.H.; Stampanoni, M.; Müller, R. The importance of murine cortical bone microstructure for microcrack initiation and propagation. Bone 2011, 49, 1186–1193.
39. Taylor, D.; Hazenberg, J.G.; Lee, T.C. Living with cracks: Damage and repair in human bone. Nat. Mater. 2007, 6, 263–268.
40. Buikstra, J.E. Ortner’s Identification of Pathological Conditions in Human Skeletal Remains; Elsevier: Amsterdam, The Netherlands, 2019; ISBN 9780128097380.

41. Voide, R.; Schneider, P.; Stauber, M.; Wyss, P.; Stampanoni, M.; Sennhauser, U.; van Lenthe, G.H.; Müller, R. Time-lapsed assessment of microcrack initiation and propagation in murine cortical bone at submicrometer resolution. Bone 2009, 45, 164–173.
42. Akhter, M.P.; Kimmel, D.B.; Lappe, J.M.; Recker, R.R. Effect of Macroanatomic Bone Type and Estrogen Loss on Osteocyte Lacunar Properties in Healthy Adult Women. Calcif. Tissue Int. 2017, 100, 619–630.
43. Currey, J.D. Stress Concentrations in Bone. J. Cell Sci. 1962, s3-103, 111–133.
44. McNamara, L.M.; Van Der Linden, J.C.; Weinans, H.; Prendergast, P.J. Stress-concentrating effect of resorption lacunae in trabecular bone. J. Biomech. 2006, 39, 734–741.
45. Qiu, S.; Rao, S.D.; Fyhrie, D.P.; Palnitkar, S.; Parfitt, M.A. The morphological association between microcracks and osteocyte lacunae in human cortical bone. Bone 2005.
46. Courtney, A.C.; Hayes, W.C.; Gibson, L.J. Age-related differences in post-yield damage in human cortical bone. Experiment and model. J. Biomech. 1996, 29, 1463–1471.
47. Carter, D.R.; Hayes, W.C.; Schurman, D.J. Fatigue life of compact bone-II. Effects of microstructure and density. J. Biomech. 1976, 9, 211–218.
48. Vashishth, D.; Behiri, J.C.; Bonfield, W. Crack growth resistance in cortical bone: Concept of microcrack toughening. J. Biomech. 1997, 30, 763–769.
49. Schaffler, M.B.; Radin, E.L.; Burr, D.B. Mechanical and morphological effects of strain rate on fatigue of compact bone. Bone 1989, 10, 207–214.
50. Awaji, H.; Ebisudani, M.; Choi, S.-M.; Ohashi, T. Crack Deflection Toughening Mechanism in Brittle Materials. In Fracture Resistance Testing of Monolithic and Composite Brittle Materials; ASTM International: West Conshohocken, PA, USA, 2009; pp. 137–151.
51. Gautieri, A.; Vesentini, S.; Redaelli, A.; Buehler, M.J. Hierarchical structure and nanomechanics of collagen microfibrils from the atomistic scale up. Nano Lett. 2011, 11, 757–766.
52. Travert, C.; Jolivet, E.; Sapin-De Brosses, E.; Mitton, D.; Skalli, W. Sensitivity of patient-specific vertebral finite element model from low dose imaging to material properties and loading conditions. Med. Biol. Eng. Comput. 2011, 49, 1355–1361.
53. Christen, D.; Webster, D.J.; Müller, R. Multiscale modelling and nonlinear.nite element analysis as clinical tools for the assessment of fracture risk. Philos. Trans. R. Soc. A Math. Phys. Eng. Sci. 2010, 368, 2653–2668.
54. Dagan, D.; Be'ery, M.; Gefen, A. Single-trabecula building block for large-scale finite element models of cancellous bone. Med. Biol. Eng. Comput. 2004, 42, 549–556.

55. Van Rietbergen, B.; Odgaard, A.; Kabel, J.; Huiskes, R. Relationships between bone morphology and bone elastic properties can be accurately quantified using high-resolution computer reconstructions. J. Orthop. Res. 1998, 16, 23–28.
56. Niebur, G.L.; Feldstein, M.J.; Yuen, J.C.; Chen, T.J.; Keaveny, T.M. High-resolution finite element models with tissue strength asymmetry accurately predict failure of trabecular bone. J. Biomech. 2000, 33, 1575–1583.
57. Ilic, S.; Hackl, K.; Gilbert, R. Application of the multiscale FEM to the modeling of cancellous bone. Biomech. Model. Mechanobiol. 2010, 9, 87–102.
58. Wolff, J. The Law of Bone Remodeling; Springer: Berlin/Heidelberg, Germany, 1986.
59. Sen, C.; Prasad, J. Exploring conditions that make cortical bone geometry optimal for physiological loading. Biomech. Model. Mechanobiol. 2019, 18, 1335–1349.
60. Lengsfeld, M.; Schmitt, J.; Alter, P.; Kaminsky, J.; Leppek, R. Comparison of geometry-based and CT voxel-based finite element modelling and experimental validation. Med. Eng. Phys. 1998, 20, 515–522.
61. Webster, D.; Müller, R. In silico models of bone remodeling from macro to nano-from organ to cell. Wiley Interdiscip. Rev. Syst. Biol. Med. 2011, 3, 241–251.
62. Hambli, R. A quasi-brittle continuum damage finite element model of the human proximal femur based on element deletion. Med. Biol. Eng. Comput. 2013, 51, 219–231.
63. Robinson, D.L.; Jiang, H.; Song, Q.; Yates, C.; Lee, P.V.S.; Wark, J.D. The application of finite element modelling based on clinical pQCT for classification of fracture status. Biomech. Model. Mechanobiol. 2019, 18, 245–260.
64. Viceconti, M.; Taddei, F.; Van Sint Jan, S.; Leardini, A.; Cristofolini, L.; Stea, S.; Baruffaldi, F.; Baleani, M. Multiscale modelling of the skeleton for the prediction of the risk of fracture. Clin. Biomech. 2008, 23, 845–852.
65. Cowin, S. Bone stress adaptation models. J. Biomech. Eng. 1993, 115, 528–533.
66. Schileo, E.; Taddei, F.; Malandrino, A.; Cristofolini, L.; Viceconti, M. Subject-specific finite element models can accurately predict strain levels in long bones. J. Biomech. 2007, 40, 2982–2989.
67. Taddei, F.; Schileo, E.; Helgason, B.; Cristofolini, L.; Viceconti, M. The material mapping strategy influences the accuracy of CT-based finite element models of bones: An evaluation against experimental measurements. Med. Eng. Phys. 2007, 29, 973–979.
68. Imai, K.; Ohnishi, I.; Bessho, M.; Nakamura, K. Nonlinear finite element model predicts vertebral bone strength and fracture site. Spine 2006, 31, 1789–1794.

69. Harrison, N.M.; McDonnell, P.; Mullins, L.; Wilson, N.; O'Mahoney, D.; McHugh, P.E. Failure modelling of trabecular bone using a non-linear combined damage and fracture voxel finite element approach. Biomech. Model. Mechanobiol. 2013, 12, 225–241.
70. Jensen, K.; Mosekilde, L. A model of vertebral trabecular bone architecture and its mechanical properties. Bone 1990, 11, 417–423.
71. Boutroy, S.; Van Rietbergen, B.; Sornay-Rendu, E.; Munoz, F.; Bouxsein, M.L.; Delmas, P.D. Finite element analysis based on in vivo HR-pQCT images of the distal radius is associated with wrist fracture in postmenopausal women. J. Bone Miner. Res. 2008, 23, 392–399.
72. Carbonare, L.D.; Valenti, M.; Bertoldo, F.; Zanatta, M.; Zenari, S.; Realdi, G.; Cascio, V.L.; Giannini, S. Bone microarchitecture evaluated by histomorphometry. Micron 2005, 36, 609–615.
73. van Rietbergen, B.; Weinans, H.; Huiskes, R.; Odgaard, A. A new method to determine trabecular bone elastic properties and loading using micromechanical finite-element models. J. Mech. 1995, 28, 69–81.
74. Bouxsein, M.L.; Boyd, S.K.; Christiansen, B.A.; Guldberg, R.E.; Jepsen, K.J.; Müller, R. Guidelines for assessment of bone microstructure in rodents using micro-computed tomography. J. Bone Miner. Res. 2010, 25, 1468–1486.
75. Pistoia, W.; Lill, C.A.; Eckstein, F.; Rietbergen, B.V.A.N.; Lochmu, E.; Ru, P. Estimation of Distal Radius Failure Load With Micro-Finite Element Analysis Models Based on Three-dimensional Peripheral Quantitative Computed Tomography Images. Bone 2002, 30, 842–848.
76. Webster, D.; Schulte, F.A.; Lambers, F.M.; Kuhn, G.; Müller, R. Strain energy density gradients in bone marrow predict osteoblast and osteoclast activity: A finite element study. J. Biomech. 2015, 48, 866–874.
77. Donaldson, F.; Ruffoni, D.; Schneider, P.; Levchuk, A.; Zwahlen, A.; Pankaj, P.; Müller, R. Modeling microdamage behavior of cortical bone. Biomech. Model. Mechanobiol. 2014, 13, 1227–1242.
78. Nalla, R.; Kruzic, J.; Kinney, J.; Ritchie, R.O. Mechanistic aspects of fracture and R-curve behavior in human cortical bone. Biomaterials 2005, 26, 217–231.
79. Thurner, P.J.; Wyss, P.; Voide, R.; Stauber, M.; Stampanoni, M.; Sennhauser, U.; Müller, R. Time-lapsed investigation of three-dimensional failure and damage accumulation in trabecular bone using synchrotron light. Bone 2006, 39, 289–299.
80. Hammond, M.A.; Wallace, J.M.; Allen, M.R.; Siegmund, T. Mechanics of linear microcracking in trabecular bone. J. Biomech. 2019, 83, 34–42.
81. Demirtas, A.; Ural, A. Material heterogeneity, microstructure, and microcracks demonstrate differential influence on crack initiation and propagation in cortical bone. Biomech. Model.

Mechanobiol. 2018, 17, 1415–1428.

82. Stipsitz, M.; Zysset, P.K.; Pahr, D.H. Efficient materially nonlinear μ FE solver for simulations of trabecular bone failure. Biomech. Model. Mechanobiol. 2020, 19, 861–874.
83. Dubey, D.K.; Tomar, V. Microstructure dependent dynamic fracture analyses of trabecular bone based on nascent bone atomistic simulations. Mech. Res. Commun. 2008, 35, 24–31.
84. Libonati, F.; Nair, A.K.; Vergani, L.; Buehler, M.J. Fracture mechanics of hydroxyapatite single crystals under geometric confinement. J. Mech. Behav. Biomed. Mater. 2013, 20, 184–191.
85. Tai, K.; Dao, M.; Suresh, S.; Palazoglu, A.; Ortiz, C. Nanoscale heterogeneity promotes energy dissipation in bone. Nat.Mater. 2007, 6, 454–462.
86. Hamed, E.; Jasiuk, I.; Yoo, A.; Lee, Y.H.; Liszka, T. Multi-scale modelling of elastic moduli of trabecular bone. J. R. Soc. Interface 2012, 9, 1654–1673.
87. Kwon, Y.W.; Clumpner, B.R. Multiscale modeling of human bone. Multiscale Multidiscip. Model. Exp. Des. 2018, 1, 133–143.